One-Dimensional Plasma Model

John Dawson

Citation: The Physics of Fluids **5**, 445 (1962); doi: 10.1063/1.1706638
View online: http://dx.doi.org/10.1063/1.1706638
View Table of Contents: http://aip.scitation.org/toc/pfl/5/4
Published by the American Institute of Physics

One-Dimensional Plasma Model

JOHN DAWSON
Plasma Physics Laboratory, Princeton University, Princeton, New Jersey
(Received June 27, 1961; revised manuscript received December 27, 1961)

A one-dimensional plasma model consisting of a large number of identical charge sheets embedded in a uniform fixed neutralizing background is investigated by following the sheet motions on a high-speed computer. The thermalizing properties and ergodic behavior of the system are examined and found to be in agreement with the assumption that one is equally likely to find the system in equal volumes of the available phase space. The velocity distribution, Debye shielding, drag on fast and slow sheets, diffusion in velocity space, the Landau damping of the Fourier modes, the amplitude distribution function for the Fourier modes, and the distribution of electric fields felt by the sheets were obtained for the plasma in thermal equilibrium and compared with theoretically predicted values. In every case, except one, the drag on a slow sheet, the numerical results agreed with theory to within the statistical accuracy of the results. The numerical results for the drag on a slow sheet were about a factor of 2 lower than the theory predicated indicating that the approximations made in the theory are not entirely valid. An understanding of the cause of the discrepancy might lead to a better understanding of collisional processes in plasmas.

INTRODUCTION

IT often occurs in physics that one can obtain an insight into the behavior of a complicated system by investigating simple models which exhibit some of the properties of the system of interest. It is the purpose of this paper to describe such a model for a plasma, and to give examples of some of the things which can be done with it.

The model is that of a one-dimensional plasma. In essence, it is a system composed of a large number of identical charge sheets embedded in a uniform fixed neutralizing background. The sheets are constrained to be perpendicular to the x axis and to move only in the x direction. They are allowed to pass freely through one another. The sheets may be viewed as point charges in one dimension and thus this model is a one-dimensional plasma.

This model exhibits a number of real-plasma properties. The forces between sheets are long range, and because of this the model exhibits collective motions as well as individual particle (sheet) motions. Each of the sheets surrounds itself with a Debye-shielding cloud; the Fourier modes exhibit Landau damping.

The model is sufficiently simple so that the motions of systems containing more than 1000 sheets can be followed in detail on a high-speed computing machine. Statistical mechanics may be applied to systems of this size. We may thus obtain statistical theories for the behavior of the system. The predictions of such theories may be compared with the machine results, and we may thus check such theories and the assumptions which go into them. Further, we have complete control of the initial state of the plasma and we can obtain as complete information as we desire about the motion of the system. The theoretical predictions may thus be checked in more complete detail than is possible with a real plasma.

Other authors have used electronic computers to solve problems in statistical mechanics. Many of these calculations have been involved with equilibrium properties.[1-4] However, some nonequilibrium calculations have been made on systems composed of particles which interact through short-range forces.[5]

MODEL

There are three equivalent versions of the one-dimensional plasma model. Two of these have been given elsewhere.[6] However, for completeness they will also be described here. The first of these has already been mentioned and is illustrated in Fig. 1. It consists of a number of identical charge sheets embedded in a fixed neutralizing background. We let the charge and mass per unit area be $-en_0\ \delta$ and $mn_0\ \delta$, where $-e$ and m are the electron charge and mass, and δ is the intersheet spacing. The background charge density is n_0e. If we wish to make a

[1] A. W. Rosenbluth, M. N. Rosenbluth, A. H. Teller, and E. Teller, J. Chem. Phys. 21, 1087 (1953).
[2] M. N. Rosenbluth and A. W. Rosenbluth, J. Chem. Phys. 22, 881 (1954).
[3] W. W. Wood and F. R. Parker, J. Chem. Phys. 27, 720 (1957).
[4] B. J. Alder, S. P. Frankel, and V. A. Lewinson, J. Chem. Phys. 23, 417 (1955).
[5] Work by B. J. Alder and T. Wainwright described in C. Kittel, *Elementary Statistical Physics* (John Wiley & Sons, Inc., New York, 1958).
[6] J. M. Dawson, Project Matterhorn Rept. MATT-31 (1960).

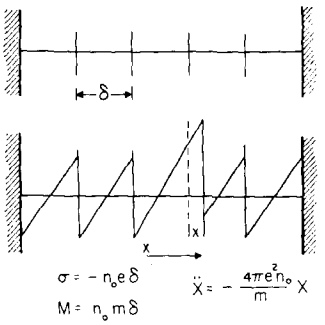

FIG. 1. One-dimensional plasma model.

correspondence between this plasma and a real plasma we must take n_0 to be the number density of the electrons.

When the system is in its equilibrium state the sheets are at rest and equally spaced. The electric field then has the sawtoothed shape shown in Fig. 1. At each sheet it jumps by $-4\pi e n_0 \delta$. In between sheets it varies linearly with distance due to the background charge.

When a sheet is in its equilibrium position the average electric field which it sees is zero. If it is displaced a distance X from its equilibrium position it passes over an amount of positive charge equal to en_0X. Let us take X positive for the sake of argument. Then if the sheet does not cross any other sheet it will see a net positive charge per unit area equal to en_0X on its negative side and a net charge $-en_0X$ per unit area on its positive side. Gauss' law then gives for the electric field which it feels

$$E = 4\pi e n_0 X. \tag{1}$$

The equation of motion of the sheet is thus given by

$$n_0 m\, \delta\ddot{X} = -4\pi e^2 n_0\, \delta X,$$

or

$$\ddot{X} = -\omega_p^2 X, \tag{2}$$

with

$$\omega_p^2 = 4\pi e^2 n_0/m.$$

For small noncrossing displacements each sheet performs simple harmonic motion about its equilibrium position, independent of what all the other sheets are doing. For noncrossing situation the system is equivalent to the system of noninteracting oscillators considered by Goldstein and Lepkin,[7] and hence exhibits the same collective modes they found.

When a sheet crosses other sheets the situation is no longer so simple. Nevertheless, we may obtain an expression similar to (2) which determines its motion. We observed that under small displacements each sheet behaved like a harmonic oscillator bound to its equilibrium position. There is one equilibrium position per sheet. Now when two sheets cross we may view them as exchanging equilibrium positions or centers of attraction. Thus the equation of motion for a sheet is the following:

$$\ddot{x} = -\omega_p^2 X. \tag{3}$$

Here x is the actual position of the sheet and X is the displacement from its instantaneous equilibrium position.

It is now possible to construct a second one-dimensional plasma model. Suppose that instead of having sheets which pass freely through one another we had perfectly elastic sheets. Now it is a property of perfectly elastic collisions between identical particles in one dimension that the particles simply exchange velocities. This leads to the same situation that results from the particles passing through each other. The only difference between the end results is the names of the particles.

It is possible to build a mechanical model of the one-dimensional plasma. It consists of a number of identical pendulums which are lined up and constrained to oscillate only along this line of centers.

One can illustrate a number of properties of the one-dimensional plasma with this model. For example, if the first pendulum is pulled aside and released so as to strike the second it will give its velocity to the second, the second in turn gives its velocity to the third and so on. A pulse thus moves through the pendulums. When a pendulum strikes its neighbor it gives up its velocity, but not its displacement. Thus the pulse leaves the pendulum behind it in a displaced state and they start to oscillate. This is equivalent to the excitation of a plasma oscillation by a fast sheet moving through a plasma.

The third model is based on the second. Suppose we have a system containing N pendulums. Consider now an N-dimensional space in which the displacement of the ith pendulum is represented by the value of the ith coordinate. The N pendulums are equivalent to an N-dimensional oscillator in this space. Now the pendulums are constrained by the conditions that the ith cannot cross the $(i+1)$st. Thus the system satisfies conditions

$$X_i \leq X_{i+1} + \delta, \qquad X_1 \geq -\delta, \qquad X_N \leq \delta, \tag{4}$$

where δ is the spacing between pendulums, and the last two conditions are imposed by the ends. The

[7] S. Goldstein and H. J. Lepkin, Ann. Phys. (N. Y.) **6**, 301 (1959).

equal signs give a set of surfaces [$(N-1)$-dimensional hyperplanes] which the system cannot cross. These walls form a closed polyhedron in N dimensions inside of which the N-dimensional oscillator is constrained to move. When two pendulums strike each other the oscillator strikes one of the walls of the polyhedrons. It rebounds elastically, i.e., its velocity perpendicular to the wall is reversed.

It is convenient to introduce the Fourier modes at this point. To do this consider the linear transformations

$$A_j = \left(\frac{2}{N+1}\right)^{\frac{1}{2}} \sum_{i=0}^{N+1} X_i \sin\left(\frac{\pi j i\ \delta}{L}\right), \tag{5}$$

$$X_i = \left(\frac{2}{N+1}\right)^{\frac{1}{2}} \sum_{j=0}^{N+1} A_j \sin\left(\frac{\pi j i\ \delta}{L}\right). \tag{6}$$

Here i refers to the ith pendulum and j to the jth Fourier mode. The walls, particles 0 and $N+1$, are considered part of the system but are held fixed. Equation (5) is an orthogonal transformation from the X_i's to the A_j's. The A_j's are in fact the same as the normal coordinate for the problem of N identical mass points connected by identical massless springs.[8] Since Eqs. (5) and (6) are the equations for an orthogonal transformation they represent a rotation of the coordinate axis.

The A_j's do not quite correspond to the usual Fourier modes. The quantity $i\delta$ is the equilibrium position of the ith pendulum. Thus these are the Fourier modes of the system in terms of Lagrangian coordinates. The usual Fourier modes are expressed in terms of Eulerian coordinates or actual positions. As long as the displacements are small compared to the wavelength of the mode ($\lambda = 2L/j$) the two are almost the same.

THERMALIZATION, ERGODIC BEHAVIOR, AND RECURRENCE TIME

The first problem that is of interest is whether or not one can apply statistical mechanics to this model; that is, whether or not this model behaves roughly ergodically. For motions with small amplitudes where crossing does not take place, the system clearly does not thermalize. On the other hand, when crossing does take place there is an exchange of energy between sheets and we may expect thermalization.

If the average energy per sheet is kept constant and the number of sheets in the system becomes very large, then we can always find motions of the system which do not exhibit crossing. These are motions in which neighboring sheets perform similar motions. These motions do not thermalize and they cannot be reached from states which do show crossing. Thus a region of phase space which is consistent with energy is unavailable. However, if the average displacement of a sheet is large compared to the intersheet spacing then the volume of the phase space in which crossing does not take place is small compared to the total phase space consistent with the energy. This is because noncrossing modes require that neighboring sheets have nearly identical motions.

We can estimate the ratio of the volumes available to crossing modes and noncrossing modes in the following way. Let us consider only the velocity space and assume the potential energy is negligible. The space available to the crossing modes is essentially all the velocity space which is consistent with the energy. This is the surface of the N-dimensional sphere with radius v,

$$v = (2\mathcal{E}_{\text{tot}}/m), \tag{7}$$

where $\mathcal{E}_{\text{tot}}$ is the total energy of the system. This volume τ_T is given by

$$\begin{aligned}\tau_T &= \frac{2(\pi)^{\frac{1}{2}N}}{\Gamma(\frac{1}{2}N)}\left(\frac{2\mathcal{E}_{\text{tot}}}{m}\right)^{\frac{1}{2}(N-2)} \\ &\cong 2(2e\pi)^{\frac{1}{2}(N-2)}(\langle V^2\rangle)^{\frac{1}{2}(N-2)}.\end{aligned} \tag{8}$$

Here $\langle V^2\rangle$ is the average square velocity of a particle.

To obtain the volume available to noncrossing modes consider the $N-1$ variables ξ_i given by

$$\xi_i = X_i - X_{i-1}. \tag{9}$$

From (2) we see that the ξ_i's satisfy oscillator equations for noncrossing motions.

$$\ddot{\xi}_i = -\omega_p^2 \xi_i. \tag{10}$$

It follows directly that the quantity Q is a constant of the motion.

$$Q_i = \dot{\xi}_i^2 + \omega_p^2 \xi_i^2. \tag{11}$$

Now ξ_i must be less than δ (the intersheet spacing) for all time if crossing is not to take place. This is true only if Q_i satisfies (12), and this means ξ_i must satisfy (13).

$$Q_i < (\omega_p\ \delta)^2, \tag{12}$$

$$|\xi| < (\omega_p\ \delta). \tag{13}$$

The volume τ_{nc} in velocity space available to noncrossing modes is thus of the order of the volume of an $(N-1)$-dimensional cube with dimension given by (13). Its volume τ_{nc} is

$$\tau_{nc} \simeq (2\ \delta\omega_p)^{(N-1)}. \tag{14}$$

[8] J. W. S. Rayleigh, *The Theory of Sound* (Dover Publications, Inc., New York, 1945), Vol. 1, pp. 172–176.

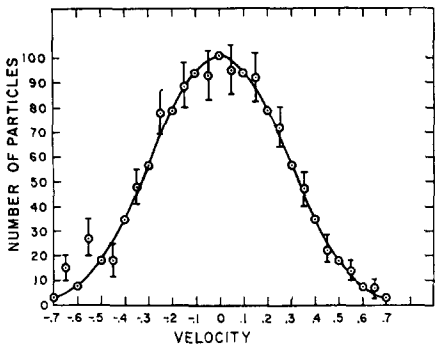

FIG. 2. Average velocity distribution function for a 9-sheet system.

Taking the ratio of τ_{nc} to τ_T gives

$$\frac{\tau_{nc}}{\tau_T} = 2\left(\frac{2}{e\pi}\right)^{\frac{1}{2}(N-2)}\left(\left\langle\frac{\omega_p^2\,\delta^2}{V^2}\right\rangle\right)^{\frac{1}{2}(N-2)} \propto \left(\frac{\delta}{D}\right)^N, \tag{15}$$

where D is the Debye length,

$$D = (kT/4\pi e^2 n_0)^{\frac{1}{2}} = (\langle V^2\rangle/\omega_p^2)^{\frac{1}{2}}, \tag{16}$$

if the plasma is in thermal equilibrium. If the Debye length is several intersheet spacings and N is of the order of hundreds this ratio is indeed small and τ_{nc} can be neglected provided there is crossing.

While this argument shows that the phase space available to noncrossing modes is negligible it does not show that the system will thermalize. In order to investigate thermalization and recurrence times, systems containing five and nine sheets were followed for 60 oscillations times ($120\pi/\omega_p$). Both systems were started out with all the energy in the first Fourier mode. The amplitude was taken sufficiently large so that crossing took place. The state of the system was printed out 120 times or twice per oscillation.

We may estimate the portion of the time these systems should spend in a state in which the first Fourier modes has more than 95% of the energy (the 95% state). Again consider only the velocity. Let the total kinetic energy of the system at time t be KE(t). The velocity spaces available to the systems are the surfaces of 5- and 9-dimensional spheres with radii ρ_v,

$$\rho_v = [2\mathrm{KE}(t)/m]^{\frac{1}{2}}. \tag{17}$$

If the first mode has all the kinetic energy then

$$A_1 = \pm\rho_v, \qquad A_j = 0, \qquad j \neq 1.$$

If we require that the kinetic energy of the first mode be 95% or more of the total kinetic energy, then we are restricted to small regions of the energy surfaces about these points. These regions can be approximated by small 4- and 8-dimensional spheres with radii Δv,

$$\Delta v = [2\mathrm{KE}(t)/20m]^{\frac{1}{2}}. \tag{18}$$

The ratio r of their volume to the surface area of the total spheres are given by

$$\begin{aligned} r_5 &= \frac{6}{16}\left(\frac{1}{20}\right)^2 \simeq 10^{-3}, \qquad 5 \text{ sheets}, \\ r_9 &= \frac{105}{768}\left(\frac{1}{20}\right)^4 \simeq 10^{-6}, \qquad 9 \text{ sheets}. \end{aligned} \tag{19}$$

If we assume the potential is negligible and that the motion is ergodic then (19) gives the portion of the time for which the mode has more than 95% of the energy. The potential energy is not quite negligible. It averaged about 20% of the total energy for the 5-sheet case and about 13% for the 9-sheet case. However, the maximum amplitude allowed the jth Fourier mode by the constraints (4) is proportional to $[\sin(j\pi/2N)]^{-1}$. Thus the first Fourier mode is allowed the largest amplitude, and most of the potential energy is in this mode. Because of this we can expect that the potential will not greatly influence the estimates given by (19) and it is possible it will even increase the portion of the time the system spends in the 95% state.

Out of the 120 samplings, the 5-sheet system was found to return to the 95% state once. This occurred after about 45 oscillation times. At that time the potential and kinetic energies of the first mode were 38 and 57%, respectively, of the total energy. This is somewhat more often than we might expect, but is not impossible in view of the crudeness of the theory and the smallness of the sample.

The 9-sheet system never returned to the 95% state during the time it was followed, and in fact the first mode never got more than 50% of the energy after the initial transients. This is in agreement with the statistical arguments.

Figures 2 and 3 show much stronger evidence of the accuracy of the statistical approximation. Figure 2 shows the time summed velocity distribution for the 9-sheet case. With so few sheets, we could not hope to obtain a smooth velocity distribution function at any one time. However, we can expect that the sum of the velocity distributions at a great many times will be accurate. The curve shown in Fig. 2 is the theoretical curve obtained if we assume that the energy available for kinetic energy is equal to the total energy minus the average potential energy. It is proportional to the area on the energy sphere one obtains if a given particle has velocity between v and $v + dv$. Its formula is

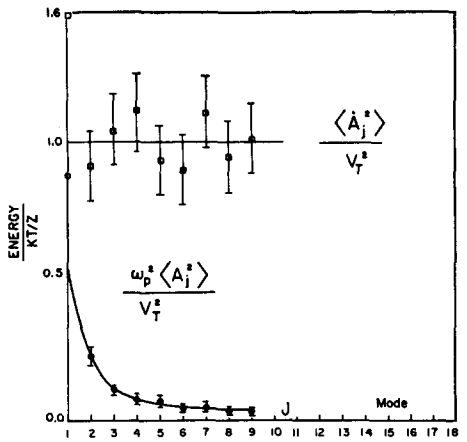

FIG. 3. Average kinetic and potential energies in the Fourier modes for a 9-sheet system.

$$F(v) \propto [1 - mv^2/2(\mathcal{E}_{tot} - \langle\phi\rangle)]^3, \qquad (20)$$

where $\mathcal{E}_{tot}$ is the total energy and $\langle\phi\rangle$ is the average potential energy. Since the average potential energy amounts to only 13% of the total energy it is almost negligible and the above approximation is not bad. Similar agreement is obtained for the 5-sheet case.

Figure 3 shows the average potential and kinetic energies of the Fourier modes for the 9-sheet case. The straight line through the kinetic-energy points is the average kinetic energy ($\frac{1}{2}KT$), while the curve through the potential-energy points is a theoretical curve whose derivations will be given later. It will be observed that all the points fall near their predicted values except for the first mode. It has about 1.5 times the predicted average kinetic and potential energies. There are several possible causes of this. The most probable one is that the system was started out with all the energy in the first mode and the finite relaxation time for the plasma resulted in the mode having a higher than average energy.

On the whole these results indicate that statistical arguments can be applied to this model. We can expect the agreement to be even better for systems containing a larger number of particles. In the next section the theoretically predicted properties of large systems are compared with the calculated properties. The excellent agreement found there is further justification for the application of statistical mechanics to the model.

PROPERTIES OF THE ONE-DIMENSIONAL PLASMA IN THERMAL EQUILIBRIUM

We may now investigate the properties of the one-dimensional plasma near thermal equilibrium. Some properties which are of interest and which will be investigated here are the following:

(1) The velocity distribution;
(2) Debye shielding;
(3) Drag on fast (supersonic) and slow (subsonic) sheets, and diffusion in velocity space;
(4) Drag on a Fourier mode (Landau damping);
(5) Amplitude distribution function for the Fourier modes;
(6) Distribution of displacements from instantaneous equilibrium position, or of the electric fields felt by the sheets.

Theories which give these properties can be developed. This section is devoted to the comparison of such theories with the machine results. It will be divided into subsections each of which deals with one of the properties. The theory of each property will be given when it is not standard.

The numerical results used for comparison were obtained by starting the system off in essentially thermal equilibrium. Because the system contained only a finite number of sheets it was impossible to start with an exact Maxwell distribution. Therefore, the particles were distributed among 16 uniformly spaced velocity groups; the number of particles in a group was proportional to exp $(-V^2/2V_T^2)$, where V was the velocity of the group. The velocity of a particle i was chosen randomly in the following way. The velocities of all the particles were put on IBM cards which were thoroughly shuffled. The resultant deck was used to give the initial velocities of the sheets. All sheets were started at their equilibrium positions.

A. Velocity Distribution

The velocity distribution of the sheets should be Maxwellian. Figure 4 shows the time summed velocity distribution for a system of 1000 sheets with a mean square velocity of 26.67 $\delta^2\omega_p^2$. This velocity gives a Debye length of 5.16 δ, $[(\langle V_T^2\rangle/\omega_p^2)^{\frac{1}{2}}]$, or a little over five intersheet spacings. The smooth curve is the theoretical Maxwell distribution obtained by assuming the energy available for velocity was equal to the total energy minus the average potential energy. Since the total potential energy should fluctuate only slightly, this should be a good approximation. Further the average potential amounted to only 8% of the total energy, so that this correction was small in any case.

The agreement between the numerical results and the theoretical curve is good. However, it is not as good as would be expected if the samples taken at different times were statistically independent. The error in this case would be of the order of $[N(V)\,\Delta V]^{\frac{1}{2}}$ and is indicated by the error bars. In these calcu-

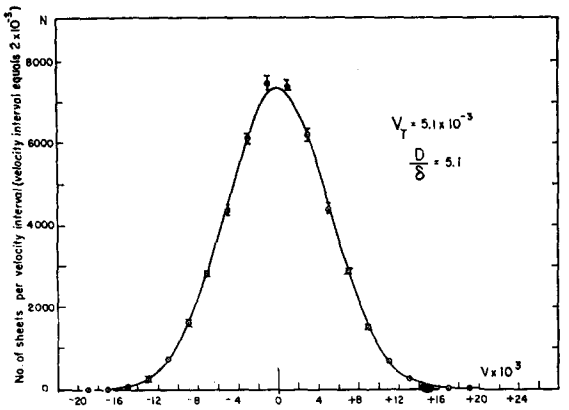

FIG. 4. Average velocity distribution function for a 1000-sheet system.

lations the system was sampled three times per plasma period $2\pi/\omega_p$. The relaxation time (the time required for a Maxwell distribution to be re-established after a small perturbation) is of the order of $[(2\pi)^{\frac{1}{2}}D/\delta\omega_p]$ as will be discussed in the section on the relaxation time. Two samples must be separated in time by more than a relaxation time if they are to be statistically independent. The system was sampled roughly six times during a relaxation time and thus the expected deviations should be of order $[6N(V)\ \Delta V]^{\frac{1}{2}}$ rather than $[N(V)\ \Delta V]^{\frac{1}{2}}$. In another calculation (1000 sheets, $D = 10.5$) for which the relaxation time was longer and in which the samples were taken more frequently (six times per oscillation), the deviations from theory were found to be even larger. However, when they were corrected for the finite relaxation time they also agreed within the expected accuracy.

Other quantities which mirrored the distribution function such as the Debye shielding cloud also showed spuriously large fluctuations about the theoretical curves when the system was sampled many times during a relaxation time. In every case, these fluctuations decreased to the expected statistical fluctuations when the sampling time became comparable with the relaxation time.

These results show that the system was constantly fluctuating about its thermal equilibrium state and that agreement with theory is not simply due to the fact that the system was started out with roughly a Maxwell distribution.

B. Debye Shielding

The Debye shielding for a 1000-sheet system with a Debye length of 5.16 intersheet spacings is shown in Fig. 5. The points are the average number of particles between 0 and 1, 1 and 2, etc., intersheet spacings from a test sheet. To obtain these averages the number of sheets within each interval was counted for every tenth sheet. This was repeated at a large number of different times and the average of the whole group found.

The smooth curve is the theoretical curve obtained from the linearized Debye theory. It is the solution of the linearized form of

$$\frac{d^2\phi}{dx^2} = -4\pi e n_0\left[\exp\left(-\frac{e\phi}{kT}\right) - 1\right] \simeq \frac{4\pi e^2 n_0\phi}{kT} = \frac{\omega_p^2}{\langle V_T^2\rangle}\phi, \tag{21}$$

$$n(x) = n_0 \exp(-e\phi/kT) \simeq n_0(1 - e\phi/kT).$$

When the boundary conditions

$$E_{\pm}(0) = (d\phi/dx) = \mp 2\pi n_0 e\delta, \qquad x = 0,$$

$$\lim_{x\to\pm\infty} E = \frac{d\phi}{dx} = 0, \tag{22}$$

are imposed, the linearized solution (23) is obtained.

$$n(x) = n_0[1 - (1/2\ D)\exp(-|x|/D)],$$

$$E = \mp 2\pi e n_0\ \delta \exp(-|x|/D), \quad \begin{matrix} -\text{for } x > 0 \\ +\text{for } x < 0 \end{matrix}$$

$$\phi = 2\pi e n_0\ \delta\ D \exp(-|x|/D). \tag{23}$$

Here D is the Debye length,

$$(kT/4\pi e^2 n_0)^{\frac{1}{2}} = \langle V_T^2\rangle/\omega_p^2, \tag{24}$$

which in this case is 5.16 δ.

It turned out that the Debye shielding was one of the more difficult quantities to obtain from the machine calculations. This was due to the fact that the statistical error in the density was of the order of $N^{\frac{1}{2}}$, where N is the number of test charges averaged over. Thus, for the above case where the maximum depression of the density is 10% we require 100 cases before the depression equals the fluctuations.

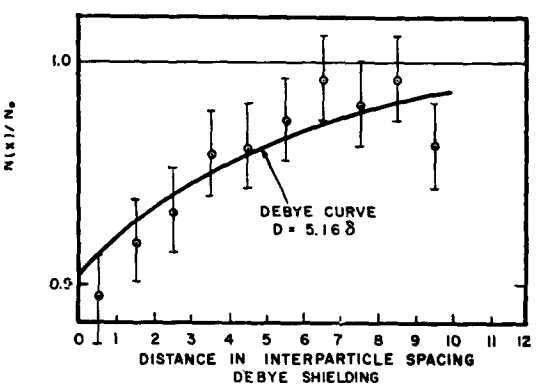

FIG. 5. Debye cloud.

To obtain the density depression of 10 percent accuracy requires 10^4 samples.

C. Drag on a Sheet and Diffusion in Velocity Space

1. *Drag on a Fast Sheet*

Let us first consider the drag on a very fast or supersonic sheet. We will take the velocity of the sheet to be positive for the sake of argument.

The plasma ahead of such a sheet cannot know of its approach. Thus, there can be no disturbance and hence no electric field ahead of the sheet. However, in going from the negative to the positive side of the sheet the electric field must jump by $-4\pi e n_0\,\delta$. Thus, the electric field behind the sheet is $4\pi e n_0\,\delta$.

The average electric field E felt by the sheet is $E = 2\pi e n_0\,\delta$, and its acceleration is given by

$$\frac{dV}{dt} = -\frac{n_0 e\,\delta E}{n_0 m\,\delta} = -\frac{\omega_p^2\,\delta}{2}. \tag{25}$$

The drag is thus independent of the velocity. It is due to the excitation of a plasma oscillation by the sheet.

Figure 6 shows a plot of the average absolute velocity as a function of time for two groups of fast particles. The initial velocity for the group represented by the circles was $2.35\ V_T$, while that for the triangles was $-2.35\ V_T$. These groups were obtained by looking for particles whose velocities lay in small velocity intervals about $\pm 2.35\ V_T$. These particles were then followed in time and the average velocities of the two groups (as functions of time) were found. The results shown are for a system of 1000 sheets with a Debye length of 10 δ. The straight line shown in Fig. 6 is the curve predicted by (25).

If the system (and hence the code) is time reversible, the drag in the negative time direction should be the same as in the forward time direction. This was found to be the case. Figure 7 shows a similar plot to 6. The data was from a 200-sheet system with a Debye length equal to 4.5 intersheet spacing. The points were obtained by looking for particles with velocities in the vicinity of 4×10^{-2}. The thermal velocity was 2.2×10^{-2}. The points show the average velocity of the group as a function of $|t - t_0|$ (t_0 was the time when we started to follow a particle). The circles are for $t - t_0$ positive while the squares are for $t - t_0$ negative. Thus the squares show the average velocity prior to the time they had velocity 4×10^{-2}.

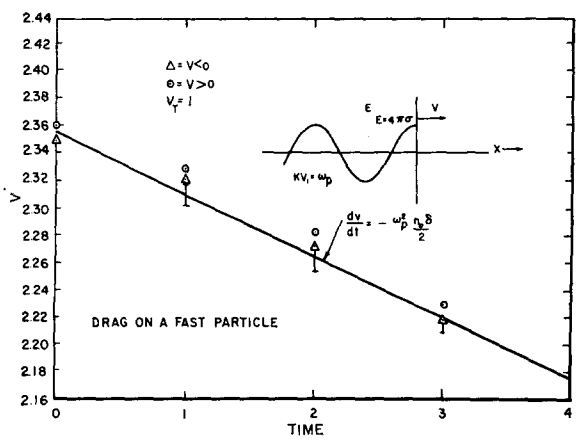

FIG. 6. The drag on a fast sheet.

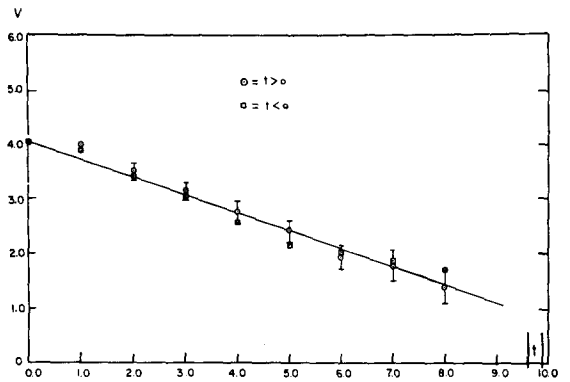

FIG. 7. The average velocity of a fast sheet as a function of the absolute time.

2. *Drag on a Slow Sheet*

Consider a sheet (test sheet) moving slowly through the plasma. Let its velocity be V. Due to its motion its Debye cloud will be distorted. It will encounter more sheets in its front than in its rear. Some of the bombarding sheets are reflected by the field surrounding it. Since more will be reflected from its front than from its rear, a slight negative charge builds up in front and a slight positive charge accumulates in its rear. The resultant field tends to slow down the sheet.

Figure 8 illustrates the distortion. The electric field will not be symmetric with respect to the sheet. Thus, if we take the potential to be zero at plus ∞ it will not be zero at $-\infty$. We will let the potential be ϕ_0 at the sheet and $\phi_{-\infty}$ at $-\infty$. We will work in the rest frame of the sheet.

The rate of change of momentum of a little element of the positive ion background is

$$n_0 e E\,\Delta x, \tag{26}$$

where Δx is the size of the element and E is the electric field which it feels.

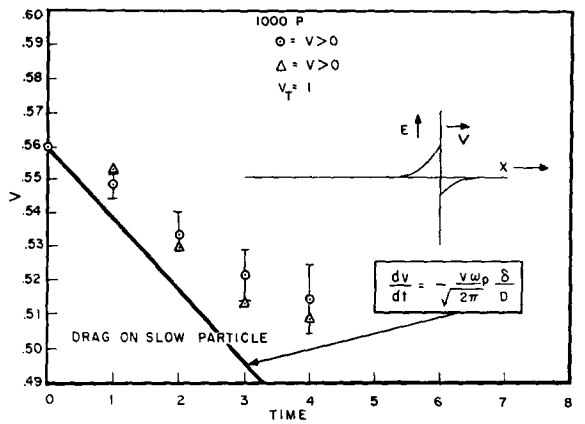

FIG. 8. The drag on a slow sheet.

Its total change in momentum in going past the sheet is

$$\delta P_i = \int n_0 e\, \Delta x E\, dt = -\int_{\infty}^{-\infty} n_0 e\, \Delta x E(x)\, \frac{dx}{-V}. \quad (27)$$

Here $-V$ is the velocity of the ions relative to the sheet. Due to the infinite mass of the ions V is constant and (27) is simply $n_0 e\, \Delta x \phi_{-\infty}/V$. In a unit time the length of column of positive ions which pass the sheet is V so that the total rate of change of the ion momentum is

$$dP_i/dt = en_0\phi_{-\infty}. \quad (28)$$

We must now find the change in momentum of the electrons (sheets). For the electrons passing through the sheet we have (29) from conservation of energy

$$v_{-\infty}^2 = v_{+\infty}^2 - (2e\phi_{-\infty}/m). \quad (29)$$

$v_{+\infty}$ and $v_{-\infty}$ are the velocities of the electron, relative to the test sheet at $\pm\infty$. For small velocities of the test sheet, $\phi_{-\infty}$ will be small; in fact it is proportional to V. Thus, for all electrons which can cross the sheet, $\phi_{-\infty}$ will be small compared to $\frac{1}{2}mv^2$. We thus find that $v_{+\infty} - v_{-\infty}$ is approximately

$$v_{+\infty} - v_{-\infty} = \Delta v = e\phi_{-\infty}/mv_{\infty+}. \quad (30)$$

From (30) we find the change in momentum of those sheets which pass over the potential barrier is given by

$$-e\phi_{-\infty}\left\{\int_{-\infty}^{\infty} f(v+V)\,dv - \int_{-(-2e\phi_0/m)^{\frac{1}{2}}}^{[-2e(\phi_0-\phi_{-\infty})/m]^{\frac{1}{2}}} f(v+V)\,dv\right\}. \quad (31)$$

The function f is the distribution function in the rest frame of the ions, and is Maxwellian. If we assume $[-2e\phi_0/m]^{\frac{1}{2}}$ is small, then we can expand f in a Taylor's series in the second integral of (31). We find that to first order in $\phi_{-\infty}$ (also V) (31) is equal to

$$-en_0\phi_{-\infty} + 2e\phi_{-\infty}f(0)[-2e\phi_0/m]^{\frac{1}{2}}. \quad (32)$$

Finally we must find the change in momentum for those sheets that are reflected by the Debye cloud. These sheets change their velocity by $-2v$ and thus their change in momentum is given by

$$m\left\{\int_{-(-2e\phi_0/m)^{\frac{1}{2}}}^{0} 2v^2 f(v+V)\,dv - \int_{0}^{[-2e(\phi_0-\phi_{-\infty})/m]^{\frac{1}{2}}} 2v^2 f(v+V)\,dv\right\}. \quad (33)$$

Making the same approximations as in (31) we find (33) is equal to (34) to first order in V or $\phi_{-\infty}$.

$$-2e\phi_{-\infty}f(0)(-2e\phi_0/m)^{\frac{1}{2}} - (-2e\phi_0/m)^2 f'(V). \quad (34)$$

Adding up (28), (32), and (34), the total change in momentum of the ions plus electrons and equating it to the negative of the rate of change of momentum of the test sheet gives

$$\frac{dP}{dt} = \frac{m\,dV}{dt} = m\left(\frac{-2e\phi_0}{m}\right)^2 f'(V) = mv_c^4 f'(V). \quad (35)$$

The quantity v_c is the minimum velocity a particle must have before it can cross the Debye cloud. If ϕ_0 is approximated by its value for V equal to zero we have

$$\phi_0 = -2\pi e n_0\, \delta D, \qquad D = V_T/\omega_p,$$

$$v_c^2 = -4\pi e n_0\, \delta D/m,$$

$$f = \frac{1}{(2\pi)^{\frac{1}{2}}V_T}\exp\left(\frac{-V^2}{2V_T^2}\right), \quad \frac{dV}{dt} = -\frac{\omega_p\,\delta}{(2\pi)^{\frac{1}{2}}D}V. \quad (36)$$

It is interesting to note that one obtains the same formula by the clothed particle approximation of Rostoker.[9] In this approximation the system is treated as one composed of particles whose interaction is given by their shielded fields. In this approximation the force per unit area on a sheet, say 1 by another, say 2 is given by

$$F = \mp 2\pi e^2 n_0^2\, \delta^2 \exp\left(\frac{|x_2 - x_1|}{D}\right), \quad \begin{matrix} - & \text{for} & x_2 > x_1 \\ + & \text{for} & x_2 < x_1 \end{matrix}. \quad (37)$$

The only sheets which impart a net momentum to the test sheet are those which are reflected from

[9] N. Rostoker, Nuclear Fusion 1, 101 (1961).

its Debye cloud. If one calculates from this model the drag on a test sheet pulled at constraint velocity through the plasma it is exactly given by (35) or (36).

Figure 8 shows the average drag on a group of particles whose initial velocity was 0.56 times the thermal velocity. The graph was obtained in a similar manner to Fig. 6 described previously. The straight line is the theoretical curve predicted by (36). As can be seen the observed drag is less by about a factor of 0.5 to 0.7. One might argue that $0.56V_T$ is not a small velocity and the difference is due to this. However, the velocity diffusion calculation that will be presented shortly gives the drag at zero velocity and it shows that the discrepancy is not due to this.

In the above calculation a number of approximations were made. First, the drag was computed as if the test sheet had an infinite mass. In reality it has the same mass as the sheets with which it is colliding. If we adopt the clothed sheet model of Rosktoker we can compute the drag for sheets of equal mass. There turns out to be two effects. First, due to the recoil of the test sheet the change in velocity of the colliding sheets is $-v$ rather than $-2v$. (v is the relative velocity of the two sheets.) Second, due to the recoil the relative velocity of a sheet with respect to the test sheet must be 2 times larger before it can cross the potential barrier. The first effect will decrease the drag by a factor of 2. However, the second effect increases the drag by a factor of 4 since it increases v_c by the factor 2 [see (35)]. Thus one would expect a net increase of a factor of 2. The numerical results, however, indicate that the drag predicted by (36) is already too large.

A number of other effects were neglected in the derivation of (36). For one, the effective mass of the sheet was assumed to be its actual mass. In reality, it would be slightly different, but this effect appears to be small (of the order of 10% for the case shown in Fig. 8).

There appears to be one possible effect which might account for the discrepancy. If one assumes that a sheet plus its Debye cloud constitute an entity and that one should add to the force on the particle the force on its Debye cloud one finds that the net force is reduced and that v_c is smaller by a factor of 2. This would correct for both the finite mass effect and the fact that (36) is already too large. Almost perfect agreement would be obtained if this were done. If two sheets are held at a fixed distance apart then (37) does indeed give the external force required to hold them there. However, the collisions which are involved here take times of the order of $1/\omega_p$, and for such rapid changes it may well be that the particle and its cloud behave like an entity. The cloud is not able to come to equilibrium with the surrounding plasma. An understanding of this discrepancy might lead to a clearer understanding of the behavior of the Debye cloud during a collision. Any effects of this type would not be so important in three dimensions since there the drag is due mainly to sideways deflection which would be only slightly affected.[9a]

3. *Diffusion in Velocity Space*

A quantity which is closely related to the drag on a sheet is the rate of diffusion in velocity space. For a system where collisions are weak these two quantities are related by the Fokker-Planck equation[10]

$$\frac{\partial f}{\partial t} + \frac{\partial}{\partial v} A(v)f(v) - \frac{1}{2}\frac{\partial^2}{\partial v^2} B(v)f(v) = 0. \tag{38}$$

Here $A(v)$ and $B(v)$ are the rate of slowing down and rate of spreading in velocity space for particles with velocity v. They are given by

$$A(v) = \lim_{\Delta t \to 0} \frac{1}{\Delta t} \int dv' \, (v' - v)P(v \mid v', \Delta t), \tag{39}$$

$$B(v) = \lim_{\Delta t \to 0} \frac{1}{\Delta t} \int dv' \, (v' - v)^2 P(v \mid v', \Delta t), \tag{40}$$

where $P(v \mid v', \Delta t)$ in the probability that a particle which has velocity v at $t = 0$ will have velocity v' at $t = \Delta t$. When the system is in equilibrium $\partial f/\partial t$ must equal zero. Thus if f is a Maxwell distribution, we obtain Eq. (41) relating $A(v)$ and $B(v)$.

$$A(v) \exp\left(\frac{-v^2}{2V_T^2}\right) - \frac{1}{2}\frac{\partial}{\partial v} B(v) \exp\left(-\frac{v^2}{2V_T^2}\right) = 0. \tag{41}$$

$B(v)$ must be a symmetric function of v so that its derivative must be zero for v equal to zero. Thus, for velocities near zero we have

$$(2V_T^2/v)A(v) = -B. \tag{42}$$

From the drag formula (36) and Eq. (42) we find that for v equal to zero B is given by

$$B(0) = [2 \, \delta V_T/(2\pi)^{\frac{1}{2}}]\omega_p^2. \tag{43}$$

[9a] *Note added in proof.* In a private communication M. Feix and O. Eldridge of General Atomic Corporation have informed the author that if one calculates the drag on a test sheet from the linearized Vlasov equations using the method of Landau[11] one obtains the correct drag for a slow sheet. The author has checked this. Where the argument given in this paper is wrong is not known.

[10] N. Wax, editor, *Selected Papers on Noise and Stochastic Processes* (Dover Publications, Inc., 1954), p. 33.

TABLE I.

V_T	δ	B_c	B_{theoret}	B_c/B_T
10.5×10^{-3}	10^{-3}	$(5.0 \pm 0.5) \times 10^{-6}$	8.4×10^{-6}	0.60
5.25×10^{-3}	10^{-3}	$(2.1 \pm 0.2) \times 10^{-6}$	4.2×10^{-6}	0.50
22.6×10^{-3}	5×10^{-3}	$(45.0 \pm 5) \times 10^{-6}$	90.4×10^{-6}	0.50

For low velocities it is much easier to measure B than A because A goes to zero with v while B does not.

Table I shows a comparison of the values found for $B(0)$ at three different temperatures with the values predicted by (43). The numerical values are 40% to 50% lower than those predicted by (43). They are in agreement with the drag found for particles with velocity $0.56V_T$.

4. *Relaxation Time*

For small departures from a Maxwell distribution the system will relax to equilibrium in a time roughly equal to the time it takes a slow particle to be stopped, or the length of time it takes a group of particles with a definite velocity to spread out into a Maxwell distribution. From (36) or (43) we find that this time is of the order of τ,

$$\tau \simeq (2\pi)^{\frac{1}{2}} D/\omega_p \delta. \tag{44}$$

There is, of course, no true relaxation time. The drag on fast particles is proportionately less than on slow particles and thus they take longer to stop. Nevertheless, (44) gives roughly the length of time a fluctuation will last or the time required for the plasma to forget the state it is in. If we want two measurements of the velocity distribution to be statistically independent, we should make them at times separated by an interval greater than τ.

D. Drag on a Fourier Mode (Landau Damping)

We may ask the question, what is the drag on a Fourier mode? Landau[11] in his treatment of plasma oscillations was the first to compute such a drag or damping for a plasma in which long-range forces dominate (short-range collisions negligible). His method and results can be applied directly to the one-dimensional plasma. For waves with phase velocities high compared to the thermal velocity the frequency ω and damping γ are given by

$$\omega^2 = \omega_p^2 + 3k^2 V_T^2, \tag{45}$$

$$\gamma = \frac{\pi}{2} \frac{\omega_p^2}{k^2} \omega \left(1 - \frac{k}{\omega} \frac{d\omega}{dk}\right) f'\left(\frac{\omega}{k}\right), \tag{46}$$

with the electric field going like

$$E = E(x)e^{(i\omega - \gamma t)}.$$

To check (45) and (46) for the one-dimensional plasma we must obtain averages similar to those used in finding the drag on a particle. However, the Fourier modes differ from the particles in that the modes behave like oscillators rather than like free particles. Their orbits in their phase planes (the A_k, $\dot{A}_k$ plane, where A_k is the amplitude of mode k) will be roughly circular. To obtain the appropriate average we proceed as follows. We mark out a small region of the phase plane and look for times (t_0's) when the mode is in this desired region. Every time we find the mode in this region we follow it forward in time for awhile. We then take averages of many such observations to obtain the average motion as a function of $t - t_0$.

One modification was made on this procedure. If we let ρ and θ be polar coordinates in the plane then it was assumed that the average orbit was a function of $\theta - \theta_0$, ρ, $t - t_0$, where θ_0 is the θ coordinate of the small region of phase space which was marked out. Thus, it was assumed that orbits starting out with different θ_0 will be similar and differ only by the phase θ_0. The average motion was found as a function of $\theta - \theta_0$ and was averaged over all θ_0 as well as t_0. Thus a ring was used for the small element of phase space. This was necessary to obtain enough samples for good statistics.

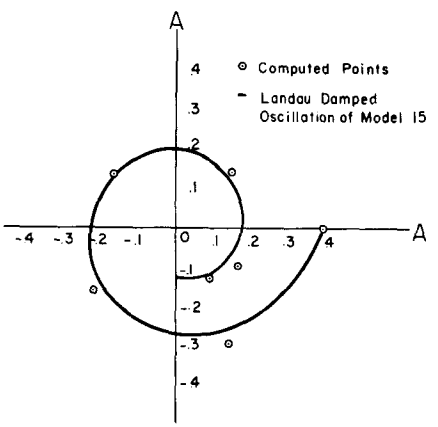

FIG. 9. The Landau damping of Fourier mode.

[11] L. Landau, J. Phys. (U. S. S. R.) **10**, 25 (1946).

Figure 9 shows the average motion of mode 15 for a 1000-sheet system with a Debye length of 10.5 intersheet spacings. The smooth curve is that predicted by the Landau theory. While the average orbit spiraled into the organ, the group spread out to fill Maxwell distribution about the organ.

The agreement is quite good and is within the statistical accuracy of the points. The orbit in the phase plane shows that not only the damping, but also the frequency is given correctly by the theory.

The wavelength for this mode was 133, ($2 \times 1000/15$), intersheet spacings, its frequency ω was $1.29\omega_p$, its phase velocity was 2.6 times the thermal velocity and its damping time was $6.7/\omega_p$.

E. Amplitude Distribution Function for the Fourier Modes

If we wish to find the amplitude distribution function for mode j for thermal equilibrium, we must evaluate the following expression:

$$P(A_j) = \frac{\int \cdots \int \exp\left(-\frac{m\omega_p^2 A_j^2}{2KT}\right) \prod_{\substack{l=1 \\ l\neq j}}^{N} dA_l \exp\left(-\frac{m\omega_p^2 A_l^2}{2KT}\right)}{\int \cdots \int \prod_{l=1}^{N} dA_l \exp\left(-\frac{m\omega_p^2 A_l^2}{2KT}\right)}. \tag{47}$$

The integration is to be carried out over the interior of the N-dimensional polyhedron bounded by the surfaces

$$X_i = X_{i+1} - \delta \tag{48}$$

(see the section on the model). We can write conditions (48) in terms of the Fourier modes by making use of Eq. (6). The constraints written in this manner are given by

$$\left(\frac{2}{N+1}\right)^{\frac{1}{2}} \sum_i A_i \left\{\sin\left[\frac{(i+1)j\pi\ \delta}{L}\right] - \sin\left(\frac{ij\pi\ \delta}{L}\right)\right\} = \left(\frac{2}{N+1}\right)^{\frac{1}{2}} \cdot \sum_i 2A_i \sin\left(\frac{j\pi\ \delta}{2L}\right) \cos\left[\frac{(i+\frac{1}{2})j\pi\ \delta}{L}\right] = \delta. \tag{49}$$

The constraints (49) give the limits of integration for (47). They are very complicated and it is not possible to work with them directly. The complication comes about because of the large number of corners and edges which the polyhedron has. These are the intersection of two or more of the surfaces given by (49).

We may try and approximate the polyhedron by a surface which rounds off the corners. If the set of equations (49) are squared and added we obtain such an average constraint. The result of this operation leads to

$$\frac{2}{N+1} \sum_{j,l,i} 4A_j A_l \sin\left(\frac{j\pi\ \delta}{2L}\right) \sin\left(\frac{l\pi\ \delta}{2L}\right) \cdot \cos\left[\frac{(i+\frac{1}{2})j\pi\ \delta}{L}\right] \cos\left[\frac{(i+\frac{1}{2})l\pi\ \delta}{L}\right] = \sum_j 4A_j^2 \sin^2\left(\frac{j\pi\ \delta}{2L}\right) = N\delta^2 = \frac{L^2}{N}. \tag{50}$$

The first equality comes from summing on i and making use of the following orthogonality relation:

$$\sum_i \cos\left[\frac{(i+\frac{1}{2})j\pi\ \delta}{L}\right] \cos\left[\frac{(i+\frac{1}{2})l\pi\ \delta}{L}\right] = \frac{N\ \delta_{jl}}{2}.$$

Here δ_{jl} is the Kronecker δ. Equation (50) is the equation for an ellipsoid. The coordinate axis A_j lies along the axis of the ellipsoid.

We can make some comparisons of the ellipsoid with the polyhedron. First the volume of the ellipsoid V_e is given by

$$V_e = \frac{L^N(\pi/4N)^{N/2}}{\Gamma[\frac{1}{2}(N+2)]} \prod_{j=1}^{N} \left[\sin\left(\frac{j\pi\ \delta}{2L}\right)\right]^{-1}. \tag{51}$$

If we take the log of (51) and approximate the sum which appears by an integral and use Sterling's approximation for the gamma function, then we find that V_e is closely approximated by (52).

$$\begin{aligned} \ln V_e &= N\left(\ln L - \ln N + \frac{1}{2}\ln\frac{e\pi}{4}\right) - \frac{2N}{\pi}\int_0^{\frac{1}{2}\pi} \ln(\sin x)\, dx \\ &= N\left(\ln\frac{L}{N} + \frac{1}{2}\ln\frac{e\pi}{4} + \ln 2\right), \\ V_e &= (e\pi)^{\frac{1}{2}N}(L/N)^N. \end{aligned} \tag{52}$$

The volume of the polyhedron V_p is given by Eq. (53):

$$V_p = \int_{-\delta}^{x_2+\delta} dx_1 \int_{-2\delta}^{x_3+\delta} dx_2 \cdots \cdot \int_{-n\delta}^{x_{n+1}+\delta} dx_n \cdots \int_{-N\delta=-L}^{\delta} dx_n. \tag{53}$$

Carrying out the integration we find

$$V_p = L^N/N! \simeq (eL/N)^N. \tag{54}$$

The ratio of the volume of the ellipsoid to the volume of the polyhedron is

$$V_e/V_p = (\pi/e)^{\frac{1}{2}N}. \tag{55}$$

If all the dimensions of the ellipsoid were shrunk by the factor $(\pi/e)^{\frac{1}{2}} = 1.075$ the ellipsoid would have the same volume as the polyhedron. Shortly, we will use the ellipsoid to compute the amplitude distribution functions for the Fourier modes. The agreement that is obtained with the computed distribution function indicates that no such correction is needed.

Another comparison we can make between the ellipsoid and the polyhedron is the distances between the origin and the points of intersection of the Fourier mode axis with the two surfaces. For the ellipsoid these distances can be obtained directly from (50) and are given by

$$d_j = \frac{L}{2N^{\frac{1}{2}} \sin (j\pi\ \delta/2L)}. \tag{56}$$

To find these distances for the polyhedron, we must find the minimum value of A_i which will satisfy the constraint conditions (49) when all other A's are zero. A close approximation to this is obtained by setting $\cos [(i + \frac{1}{2})j\pi\delta/L]$ equal to 1. We thus find

$$d_j = \left(\frac{N+1}{2}\right)^{\frac{1}{2}} \frac{\delta}{2 \sin (j\pi\ \delta/2L)} \cong \frac{L}{(2N)^{\frac{1}{2}} 2 \sin (j\pi\ \delta/2L)}. \tag{57}$$

The two quantities are the same function of j and differ only by a factor $\sqrt{2}$.

Turning again to the problem of finding $P(A_j)$ we substitute the ellipsoidal boundary given by (50) for the polyhedron surface given by (49). We will make one further approximation; that the potential energy in all modes except the jth is small compared to KT, i.e.,

$$m\omega_p^2 A_l^2/2KT \ll 1.$$

When the Debye length is large compared to the intersheet spacing this assumption will be found to be valid for almost all modes. With these two approximations the integrals appearing in the numerator of (47) simply give the volume of the $(N-1)$-dimensional ellipsoid whose equation (58) is obtained directly from (50).

$$\sum_{\substack{l \\ l \neq j}} 4A_l^2 \sin^2 \left(\frac{l\pi\ \delta}{2L}\right) = \frac{L^2}{N} - 4A_j^2 \sin^2 \left(\frac{j\pi\ \delta}{2L}\right). \tag{58}$$

The volume of this ellipsoid is given by

$$V = \left(\frac{\pi}{N-1}\right)^{\frac{1}{2}(N-1)} \frac{[L^2/N - 4A_j^2 \sin^2 (j\pi\ \delta/2L)]^{\frac{1}{2}N}}{\Gamma(\frac{1}{2}N)} \cdot \prod_{\substack{l \\ l \neq j}} \left[2 \sin \left(\frac{l\pi\ \delta}{L}\right)\right]^{-1} = C \exp [-A_j^2(2N^2/L^2) \sin^2 (j\pi\ \delta/2L)]. \tag{59}$$

The constant C depends on N but has no A_j dependence. With this value for the integral we find upon substituting in (47) that $P(A_j)$ is proportional to (60).

$$P(A_j) \propto \exp \left[-A_j^2 \left(\frac{m\omega_p^2}{2KT} + \frac{2N^2}{L^2} \sin^2 \frac{j\pi\ \delta}{2L}\right)\right]. \tag{60}$$

In the limit of small j and large L, (61) takes the form

$$P(A_j) \propto \exp \{-A_j^2[(m\omega_p^2/2KT) + \tfrac{1}{2}k^2]\}, \tag{61}$$

where $k = j\pi/L$. One also obtains (61) if one takes $P(A_j)$ to be given by

$$P(A_j) \propto e^{-\psi(A_j)/KT}, \tag{62}$$

where ψ is the potential of average force required to create the wave. It is the work done against the electrostatic and the pressure force; the pressure being given by the isothermal pressure law, P equals nKT. This approach is equivalent to that given by Bohm and Pines.[12]

The energy density due to a displacement X in this approximation is given by

$$\psi = \tfrac{1}{2}n_0 m\omega_p^2 X^2 + \tfrac{1}{2}n_0 KT(\partial X/\partial x)^2, \tag{63}$$

where the first term is the work done against the electric field and the second term is the work done against the pressure. Taking X to be equal to $(2/N)^{\frac{1}{2}}A_k \sin kx$ and integrating (64) from 0 to L gives (64) for the potential of the average force.

$$\psi = A_k^2[(n_0 m\omega_p^2 L/2N) + (k^2 n_0 KTL/2N)] = A_k^2(\tfrac{1}{2}m\omega_p^2 + \tfrac{1}{2}k^2 KT). \tag{64}$$

Substitution of (64) in (62) also gives (61) for $P(A_j)$.

The potential energy of the jth mode $[\int (E^2/8\pi)\, dx]$ is equal to $\frac{1}{2}m\omega_p^2 A_j^2$. The average value of this quantity $\langle\phi_j\rangle$ obtained from (60) is given by

$$\langle\phi_j\rangle = \left[\frac{2}{KT} + \frac{8N^2}{m\omega_p^2 L^2} \sin^2 \left(\frac{j\pi\ \delta}{2L}\right)\right]^{-1}. \tag{65}$$

Figures 10 and 11 show a comparison of formula (65) with machine results. Figure 10 shows a plot of $(2\langle\phi_j\rangle/KT)^{\frac{1}{2}}$ vs j for a 1000-sheet system with

[12] D. Pines and D. Bohm, Phys. Rev. **85**, 338 (1952).

a Debye length of 10.5 intersheet spacings. The smooth curve is the curve predicted by (65). The agreement is good for all modes beyond the tenth. The explanation of the deviation for the low modes is the following. The initial state of the plasma was such that on the average a mode has an energy of $\frac{1}{2}KT$. The low modes behave like oscillators so that if they did not couple to the rest of the plasma their average potential energy would be $\frac{1}{4}KT$. These modes couple weakly to the rest of the plasma since their phase velocity is much larger than the thermal velocity (small Landau damping). Thus the modes below 10 did not have time to come to equilibrium during the calculations.

Figure 11 shows a similar plot for large j's for a 200-sheet system with a Debye length of 4.5 intersheet spacings. The curve is that predicted by (65).

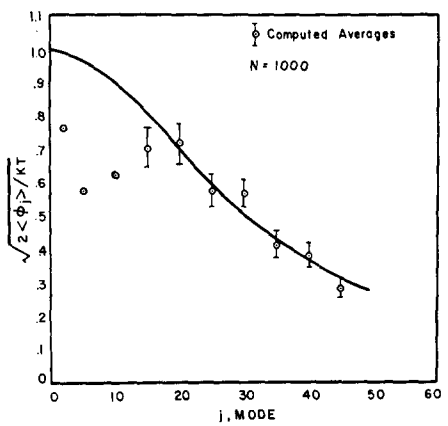

FIG. 10. The root mean square amplitude vs Fourier-mode number.

The agreement is good all the way out to the 200th mode.

For large j Eq. (60) is approximately given by

$$P(A_j) \propto \exp\{-A_j^2[(2N^2/L^2)\sin^2(j\pi/2N)]\}. \quad (66)$$

For j between $\frac{1}{2}N$ and N the width of this Gaussian varies only slightly (by the factor $\sqrt{2}$). Because of this all these modes have nearly the same probability distributions for A_j and so we can take the average amplitude distribution for these modes. Since the Fourier modes, unlike the sheets, are not identical, this rough equivalent of the high modes is important in obtaining good statistics.

Figure 12 shows the average amplitude distribution function for modes 100 to 200 for the 200-sheet system mentioned above. The smooth curve is the average Gaussian for this group. Again the agreement is very good confirming the accuracy of (60).

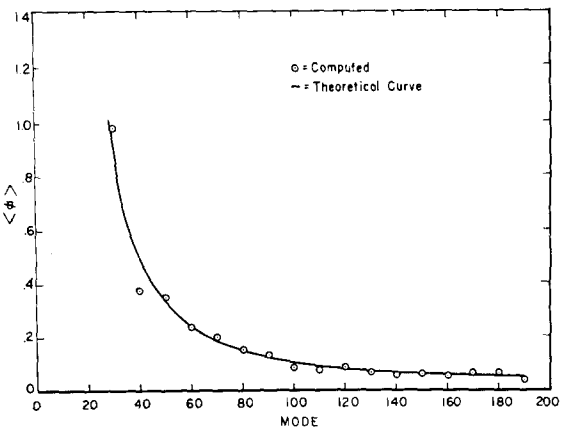

FIG. 11. Average potential energy vs Fourier-mode number.

F. Distribution of Displacements from Instantaneous Equilibrium Position or of the Electric Fields Felt by the Sheets

Let us investigate the distribution of displacements from instantaneous equilibrium position. By Eq. (1) this is equivalent to finding the probability that a sheet feels an electric field $E = 4\pi en_0X$. This problem is most easily attacked by picking out one sheet, a test sheet, and treating it like an oscillator (see the section on the model) while the other sheets are treated as a gas of freely interpenetrating sheets which, however, cannot pass through the test sheet. We will compute the potential of the average force.

Let the test sheet be displaced a distance X from its equilibrium position. By Eq. (1) the electric field at the sheet is equal to $4\pi en_0X$. The rest of

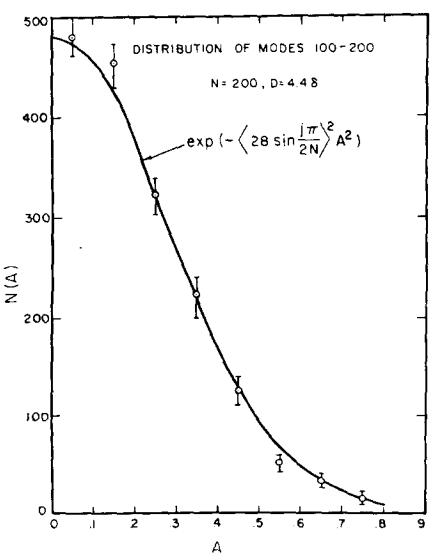

FIG. 12. Average amplitude distribution function for large J modes.

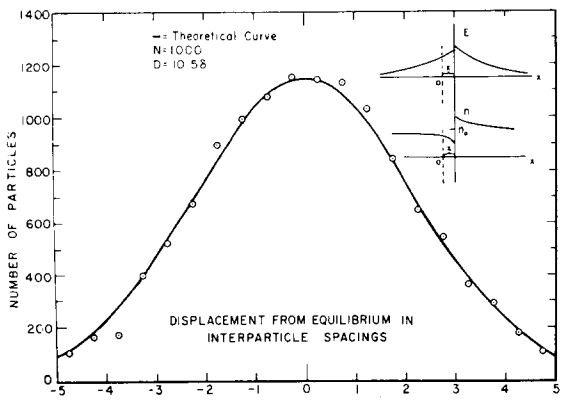

FIG. 13. Distribution of displacements from equilibrium position.

the plasma will shield itself from this electric field and the E field will die out exponentially with distance from the sheet. Taking the sheet's position (not its displacement from equilibrium) as zero, the electric field is given by

$$E = 4en_0Xe^{-|x|/D}. \tag{67}$$

Here X is the displacement from equilibrium and the field due to the sheet itself is neglected. The potential on the positive side of the sheet with respect to $+\infty$ is given by (68), while the potential on the negative side with respect to $-\infty$ is given by (69).

$$\phi_+ = +4\pi en_0X\ De^{-x/D}, \tag{68}$$

$$\phi_- = -4\pi en_0X\ De^{+x/D}. \tag{69}$$

Since there is no direct contact between the gas on both sides of the sheet we can work with these two potentials. The number densities of the gas on the positive and negative sides are

$$n_\pm = n_0 \exp\left(-\frac{e\phi_\pm}{KT}\right) \simeq n_0\left(1 - \frac{e\phi_\pm}{KT}\right). \tag{70}$$

By (68), (69), and (70) there is a jump in density across the test sheet which is equal to Δn,

$$\Delta n = n_+(0) - n_-(0) = 8n_0^2e^2X\ D/KT. \tag{71}$$

As a result there is a pressure difference across the sheet given by (72).

$$P_+ - P_- = KT(n_+ - n_-) = 2n_0\omega_p^2m\ XD. \tag{72}$$

The average force F per unit area on the sheet produced by both the electric field and the pressure jump is given by

$$F = -m\omega_p^2X(1 + 2n_0\ D), \tag{73}$$

while the potential of the average force is given by

$$\psi = \tfrac{1}{2}m\omega_p^2X^2(1 + 2n_0\ D). \tag{74}$$

The distribution of displacements from instantaneous equilibrium positions is proportional to $\exp(-\psi/KT)$ and is equal to

$$P(x) \propto \exp\left[-(\omega_p^2X^2/2V_T^2)(1 + 2n_0\ D)\right]. \tag{75}$$

Figure 13 shows a plot of $P(x)$ vs X for a system of 1000 sheets with Debye length of 10.5 δ. The smooth curve is that predicted by (75) and the agreement is within the accuracy of the numerical results.

CHECKS ON THE CALCULATIONS

A number of checks were made on the calculations. First, the conservation of energy was checked. It was found that the energy had a tendency to drift down. For the 1000-sheet system with a Debye length of 10.5 the system lost 7 parts in 1000 of its energy during 18 oscillations (2200 time steps on the machine). Each sheet was crossed by roughly 2000 other sheets during this time so that in crossing another sheet a given sheet lost on the average 3 parts in 10^6 of its energy. It was possible to increase the accuracy at the expense of speed by shortening the time step. However, this did not seem worthwhile.

Second, the motion of a 9-sheet system was reversed and found to retrace its path within an accuracy of one part in 10^3 (all orbits were this accurate) over a period of 6 oscillations.

Third, a case was run (9 sheets) when no crossing took place. These were checked against exact analytic results and found to be accurate to a few parts in 10^8 over a period of one oscillation.

Fourth, the drag on the particle was the same in the negative and positive time directions. Thus, even though the calculations had a definite direction, foward in time, the results were symmetric in time. This indicates that computational errors were small.

CONCLUSIONS

The results of these calculations and their agreement with theoretical predictions show that it is possible to check statistical theories and any approximations and assumptions which go into them by following the motion of sufficiently simple models in detail on a high-speed computer.

The good agreement between theory and computation leads to a considerable confidence in the theory. Since the theory that has been used and approximations that have been made are on the whole those which are often employed in plasma

physics, the results strongly support their validity. The only result that deviated from the theoretical prediction was that for the drag on a slow sheet. Here the deviation amounts to about 50%. It appears that the theoretical result may depend on the detailed behavior of the Debye clouds for two colliding particles.

Finally, the model should be able to serve as a useful guide for obtaining theories of nonequilibrium properties, and nonlinear phenomenon.

ACKNOWLEDGMENT

This work was performed under the auspices of the U. S. Atomic Energy Commission.

THE PHYSICS OF FLUIDS VOLUME 5, NUMBER 4 APRIL, 1962

Oscillations in a Relativistic Plasma

K. IMRE*

Department of Nuclear Engineering and Radiation Laboratory, University of Michigan, Ann Arbor, Michigan

(Received August 24, 1961; revised manuscript received October 24, 1961)

The linear oscillations in a hot plasma which is representable by the relativistic Vlasov equation with the self-consistent fields are investigated. The generalization of Bernstein's method for the relativistic case is used to obtain the formal solution of the linearized problem. Particular attention is given to the case when the system initially is in the relativistic equilibrium state. The dispersion equation is derived and studied for the case when the propagation is along the direction of the unperturbed magnetic field, considering the spatial dispersions explicitly. The asymptotic expansions are developed corresponding to the dispersion relations of the cases studied. It is found that transverse waves propagating along the unperturbed field are Landau damped if $\nu^2 \geq 1 - \Omega^2/\omega^2$, ν and Ω being the index of refraction and the gyrofrequency, respectively. In the absence of the external field the cutoff frequency, which is found to be the same for both longitudinal and the transverse modes, is shown to be a monotonically decreasing function of the temperature.

I. INTRODUCTION

IN the recent literature the problems involving the hot ionized gases have increasingly attracted the plasma investigators. The relativistic Vlasov equation together with Maxwell's equations for the self-consistent fields have been used in most of these approaches. Since the correlations are ignored as a whole in this model, the validity and applicability of this representation are somewhat restricted. The extent to which this imposes limitations has not yet been made evident in the literature. However, leaving these questions unanswered, in this paper it will be assumed that this model can properly represent the system under consideration to some extent.

Furthermore, to study the oscillatory phenomena, a linearized theory will be employed with the presence of a constant external magnetic field. As a special case, the unperturbed distribution function will be assumed to be the relativistic equilibrium distribution function. It will be shown that, taking appropriate limits of the results of the present paper, one can obtain the results of the former analyses in which, in the absence of the external field, the weakly relativistic and ultrarelativistic cases were studied using the approximate forms of the equilibrium distribution corresponding to the respective cases.

The formulation of the mathematical problem will be given in Sec. II. The derivation of the formal solution of the linearized system and the dispersion relation will be sketched subsequently. Particular attention will be given to the case in which the propagation is along the external field.

Sections III, IV, and V will be devoted to the study of the longitudinal, transverse, and the magnetohydrodynamic waves, respectively. A short discussion of the results deduced will be given in Sec. VI.

II. FORMAL SOLUTION OF THE LINEARIZED PROBLEM

The system of equations by which the plasma is assumed to be represented is given as

* Present address: Conductron Corporation, Ann Arbor, Michigan.